Experimental Validation of Robust Iterative Learning Control on an Overhead Crane Test Setup

Tong Duy Son, Goele Pipeleers and Jan Swevers

Department of Mechanical Engineering, Div. PMA, Katholieke Universiteit Leuven, Celestijnenlaan 300B, Heverlee B3001, Belgium
Email: tong.duyson@mech.kuleuven.be.

Abstract: This paper presents an experimental validation of a recently proposed robust norm-optimal iterative learning control (ILC). The robust ILC input is computed by minimizing the worst-case value of a performance index under model uncertainty, yielding a convex optimization problem. The proposed robust ILC design is experimentally validated on a lab scale overhead crane system, showing the advantages of the approach over classical ILC designs in monotonic convergence and tracking performance.

Keywords: Iterative learning control (ILC), Robust control.

1. INTRODUCTION

Iterative learning control (ILC) is widely adopted in control applications as an effective approach to improve performance of repetitive processes (Bristow et al., 2006; Ahn et al., 2007). The key idea of ILC is to update the control signal iteratively based on measured data from previous trials, such that the output converges to the given reference trajectory. Most ILC update laws use the system model as a basis for the learning algorithm. Since system models are never perfect in practical applications, accounting for model uncertainty in the ILC design and analysis is important.

The robustness of a variety of ILC approaches has been discussed in the literature: linear ILC (Longman, 2000), norm-optimal ILC (Donkers et al., 2008; Haber et al., 2012), two dimensional learning system (Rogers et al., 2001), and gradient-based ILC algorithms (Owens and Daley, 2008). In general, these papers derive ILC convergence conditions. Some papers present ILC designs that explicitly account for model uncertainty to improve robust performance. In (Moore et al., 2005), the authors consider higher order ILC, while (Bristow and Alleyne, 2008) investigate the choice of time-varying filtering. (Ahn et al., 2006) designs a robust ILC that account for interval uncertainty on each impulse response. Moreover, $\mathcal{H}_\infty$ norm based design techniques are studied in (Roover, 1996; van de Wijdeven et al., 2011).

Recently, we have proposed a robust norm-optimal ILC approach taking into account model uncertainty (Son et al., 2013). The robust control design is formulated as a min-max problem with a quadratic cost function to minimize its worst-case value under model uncertainty. Then the algorithm is reformulated as a convex optimization problem, yielding a global optimal solution. The robust ILC algorithm has shown advantages in convergence and performance analysis. In this paper, the proposed robust ILC is validated experimentally with a lab scale overhead crane system.

The paper is organized as follows. Section 2 provides the background on robustness of norm-optimal ILC. Section 3 formulates the developed robust ILC approach. Experimental results are given in Section 4, and Section 5 concludes this paper.

2. BACKGROUND

2.1 ILC System representation

The ILC design is considered in discrete time, where the discrete time instants are labeled by $k = 0, 1, \ldots$ and q denotes the forward time shift operator. The trials are labeled by the subscript $j = 0, 1, \ldots$ Each trial comprises N time samples and prior to each trial the plant is returned to the same initial conditions. The robust ILC design considers linear time-invariant (LTI), single-input single-output (SISO) systems that are subject to unstructured additive uncertainty. That is, the method accounts for a set of systems $P_\Delta(q)$ of the following form:

$$P_\Delta(q) = \hat{P}(q) + \Delta(q)W(q)\,, \quad \Delta(q) \in \mathcal{B}_\Delta\,, \tag{1a}$$

with

$$\mathcal{B}_\Delta = \{\Delta(q) = \text{stable, causal LTI system} : \|\Delta(q)\|_\infty \leq 1\}\,, \tag{1b}$$

where $\|.\|_\infty$ is the $\mathcal{H}_\infty$ norm. $\hat{P}(q)$ is the nominal plant model and the weight $W(q)$ determines the size of the uncertainty. $\hat{P}(q)$, $W(q)$, and $\Delta(q)$ are stable transfer functions. Without loss of generality, $\hat{P}(q)$ and $W(q)$ are assumed to have relative degree 1, while $\Delta(q)$ has relative degree 0. Let $\hat{p}(k)$, $\delta(k)$ and $w(k)$ denote the impulse responses of $\hat{P}(q)$, $\Delta(q)$ and $W(q)$, respectively, leading to $\hat{P}(q) = \sum_{k=1}^{N} \hat{p}(k)q^{-k}$, $\Delta(q) = \sum_{k=0}^{N-1} \delta(k)q^{-k}$, and $W(q) = \sum_{k=1}^{N} w(k)q^{-k}$. The system input in trial j is denoted by $u_j(k)$, and $y_j(k)$ is the system output.

The ILC design is formulated in the trial domain, relying on the lifted system representation (Bristow et al., 2006). The input, output and reference trajectory samples during the trial are grouped into large vectors

$$\mathbf{u}_j = [u_j(0)\ u_j(1)\ \cdots\ u_j(N-1)]^T\ ,$$
$$\mathbf{y}_j = [y_j(1)\ y_j(2)\ \cdots\ y_j(N)]^T\ ,$$
$$\mathbf{y}_\mathrm{d} = [y_d(1)\ y_d(2)\ \cdots\ y_d(N)]^T\ ,$$

and the plant dynamics are reformulated between $\mathbf{u}_j$ and $\mathbf{y}_j$:

$$\mathbf{y}_j = \mathbf{P}_\Delta\, \mathbf{u}_j\,. \tag{2}$$

Let T be the Toeplitz operator:

$$T(x_1, x_2, \ldots, x_N) := \begin{bmatrix} x_1 & 0 & \cdots & 0 \\ x_2 & x_1 & \ddots & \vdots \\ \vdots & \ddots & \ddots & 0 \\ x_N & \cdots & x_2 & x_1 \end{bmatrix}, \tag{3}$$

then $\mathbf{P}_{\boldsymbol{\Delta}}$ is given by

$$\mathbf{P}_{\boldsymbol{\Delta}} = \hat{\mathbf{P}} + \boldsymbol{\Delta}\mathbf{W}\,, \tag{4}$$

where

$$\hat{\mathbf{P}} = T(\hat{p}(1), \hat{p}(2), \ldots, \hat{p}(N))\,,$$
$$\boldsymbol{\Delta} = T(\delta(0), \delta(1), \ldots, \delta(N-1))\,,$$
$$\mathbf{W} = T(w(1), w(2), \ldots, w(N))\,.$$

In the lifted form, the set $\mathcal{B}_\Delta$ translates into the following set $\mathcal{B}_{\boldsymbol{\Delta}}$ for the matrices $\boldsymbol{\Delta}$:

$$\mathcal{B}_{\boldsymbol{\Delta}} = \{\boldsymbol{\Delta} = T(\delta(0), \ldots, \delta(N-1)) : \Delta(q) = \sum_{k=0}^{N-1} \delta(k) q^{-k}$$
$$= \text{stable, causal LTI system with } \|\Delta(q)\|_\infty \leq 1\}\,. \tag{5}$$

2.2 Robustness in Norm-optimal ILC

Norm-optimal ILC is an optimization-based ILC design, where the control signal is computed by minimizing the following performance index with respect to $\mathbf{u}_{j+1}$:

$$J(\mathbf{u}_{j+1}, \boldsymbol{\Delta}) = \|\mathbf{e}_{j+1}\|^2_{\mathbf{Q}} + \|\mathbf{u}_{j+1} - \mathbf{u}_j\|^2_{\mathbf{R}} + \|\mathbf{u}_{j+1}\|^2_{\mathbf{S}}, \tag{6}$$

where $\mathbf{Q}$, $\mathbf{R}$, $\mathbf{S}$ are symmetric positive definite matrices. We define $\|x\|^2 = x^T x$ and $\|x\|^2_\mathrm{M} = x^T \mathrm{M} x$. In the cost function, $\mathbf{e}_{j+1}$ is the $(j+1)$-th trial tracking error, $\mathbf{e}_{j+1} = \mathbf{y}_d - \mathbf{P}_{\boldsymbol{\Delta}}\mathbf{u}_{j+1}$, and is given by

$$\mathbf{e}_{j+1} = \mathbf{e}_j - (\hat{\mathbf{P}} + \boldsymbol{\Delta}\mathbf{W})(\mathbf{u}_{j+1} - \mathbf{u}_j). \tag{7}$$

In classical norm-optimal ILC, the error $\mathbf{e}_{j+1}$ is replaced by the nominal estimated error $\hat{\mathbf{e}}_{j+1}$ assuming $\boldsymbol{\Delta} = 0$. This leads to the following ILC update law:

$$\mathbf{u}_{j+1} = \boldsymbol{\mathcal{Q}}\mathbf{u}_j + \boldsymbol{\mathcal{L}}\mathbf{e}_j, \tag{8a}$$

where

$$\boldsymbol{\mathcal{Q}} = (\hat{\mathbf{P}}^T\mathbf{Q}\hat{\mathbf{P}} + \mathbf{S} + \mathbf{R})^{-1}(\hat{\mathbf{P}}^T\mathbf{Q}\hat{\mathbf{P}} + \mathbf{R}), \tag{8b}$$
$$\boldsymbol{\mathcal{L}} = (\hat{\mathbf{P}}^T\mathbf{Q}\hat{\mathbf{P}} + \mathbf{S} + \mathbf{R})^{-1}\hat{\mathbf{P}}^T\mathbf{Q}. \tag{8c}$$

Consequently, robust monotonic convergence is achieved if:

$$\|\boldsymbol{\mathcal{Q}} - \boldsymbol{\mathcal{L}}\mathbf{P}_{\boldsymbol{\Delta}}\| < 1,\ \ \forall \boldsymbol{\Delta} \in \mathcal{B}_{\boldsymbol{\Delta}}, \tag{9}$$

yielding

$$\|(\hat{\mathbf{P}}^T\mathbf{Q}\hat{\mathbf{P}} + \mathbf{S} + \mathbf{R})^{-1}(\mathbf{R} - \hat{\mathbf{P}}^T\mathbf{Q}\boldsymbol{\Delta}\mathbf{W})\| < 1,\ \ \forall \boldsymbol{\Delta} \in \mathcal{B}_{\boldsymbol{\Delta}}. \tag{10}$$

Any attempt to remove $\boldsymbol{\Delta}$ for deriving a robust monotonic convergence condition usually results in conservative results. A common approach is to increase $\mathbf{S}$ sufficiently such that (10) can be satisfied, but it then reduces the converged performance. Note that the use of $\|\mathbf{S}\| > 0$ is similar to using low-pass filter in frequency-domain ILC (Gunnarsson and Mikael Norrlöf, 2001). This compromise motivates our robust ILC design approach such that both monotonic convergence and high performance are achieved.

3. ROBUST ILC DESIGN

In our proposed robust norm-optimal ILC approach (Son et al., 2013), we consider minimizing the cost function (6) without the assumption $\boldsymbol{\Delta} = 0$. In other words, $\boldsymbol{\Delta}$ is taken into account in the cost function.

First, in order to obtain a tractable reformulation of the proposed robust ILC design, the set $\mathcal{B}_{\boldsymbol{\Delta}}$ in (5) is replaced by an outer approximation:

$$\mathcal{B}^\mathrm{o}_{\boldsymbol{\Delta}} = \left\{\boldsymbol{\Delta} \in \mathbb{R}^{N\times N} \,:\, \|\boldsymbol{\Delta}\| \leq 1\right\}, \tag{11}$$

where $\|.\|$ is the induced matrix 2-norm. Hence, we replace $\|\Delta(q)\|_\infty \leq 1$ by $\|\boldsymbol{\Delta}\| \leq 1$, and extend the set of lower triangular Toeplitz matrices to $\mathbb{R}^{N\times N}$. With the first replacement, we also extent the set $\mathcal{B}_{\boldsymbol{\Delta}}$ since for stable, causal, LTI systems $\Delta(q)$, it holds that $\|\boldsymbol{\Delta}\| \leq \|\Delta(q)\|_\infty$ (Norrlöf and Gunnarsson, 2002). In addition, equality holds for $N \to \infty$.

Next, we propose a robust norm-optimal ILC design by considering the following worst-case optimization problem:

$$\underset{\mathbf{u}_{j+1}}{\text{minimize}}\ \sup_{\|\boldsymbol{\Delta}\|\leq 1} \{J(\mathbf{u}_{j+1}, \boldsymbol{\Delta})\} \tag{12a}$$

where substituting (7) in (6) yields

$$J(\mathbf{u}_{j+1}, \boldsymbol{\Delta}) = \|\mathbf{e}_j - (\hat{\mathbf{P}} + \boldsymbol{\Delta}\mathbf{W})(\mathbf{u}_{j+1} - \mathbf{u}_j)\|^2_{\mathbf{Q}}$$
$$+ \|\mathbf{u}_{j+1} - \mathbf{u}_j\|^2_{\mathbf{R}} + \|\mathbf{u}_{j+1}\|^2_{\mathbf{S}}. \tag{12b}$$

The following results present solution and convergence properties of the proposed robust ILC approach.

Lemma 3.1. The robust ILC algorithm (12) is equivalent to the following convex optimization problem:

$$\begin{aligned} \underset{\mathbf{u}_{j+1}, \lambda_{j+1}}{\text{minimize}}\ & J_\mathrm{dual}(\mathbf{u}_{j+1}, \lambda_{j+1}) \\ \text{subject to}\ & \lambda_{j+1}\mathbf{I} - \mathbf{Q} \succeq 0 \\ & \mathbf{Q}\hat{\mathbf{e}}_{j+1} \in \mathcal{R}\left(\mathbf{Q} - \lambda_{j+1}\mathbf{I}\right), \end{aligned} \tag{13a}$$

where λ_{j+1} is a scalar variable and

$$J_\mathrm{dual}(\mathbf{u}_{j+1}, \lambda_{j+1}) = \hat{\mathbf{e}}^T_{j+1}\left(\mathbf{Q}^{-1} - \lambda^{-1}_{j+1}\mathbf{I}\right)^\dagger \hat{\mathbf{e}}_{j+1}$$
$$+ \lambda_{j+1}\|\mathbf{W}(\mathbf{u}_{j+1} - \mathbf{u}_j)\|^2 + \|\mathbf{u}_{j+1} - \mathbf{u}_j\|^2_{\mathbf{R}} + \|\mathbf{u}_{j+1}\|^2_{\mathbf{S}}. \tag{13b}$$

Proof. The derivation of (13) is elaborated in (Son et al., 2013).

Theorem 3.1. Given the nominal system model $\hat{\mathbf{P}}$ and the additive uncertainty weight $\mathbf{W}$, the robust ILC algorithm obtaining from (13) is monotonic convergent. Moreover, perfect asymptotic tracking error, i.e. $\mathbf{e}_\infty = 0$, can be achieved if there are no constraints on the input signal.

Proof. See (Son et al., 2013).

This Theorem provides the main advantage of our robust design over classical ILC, that is, the robust ILC can

achieve both monotonic convergence and high performance tracking error. Next, we consider the convergence speed.

Lemma 3.2. The proposed robust ILC algorithm (13) can be interpreted as the classical norm-optimal ILC formulation (8), except that the weight matrices $\mathbf{Q}$ and $\mathbf{R}$ are updated trial-by-trial, determined by the optimal λ_{j+1}:

$$\mathbf{Q}_{j+1}(\lambda_{j+1}) = \left(\mathbf{Q}^{-1} - \lambda_{j+1}^{-1}\mathbf{I}\right)^{\dagger} \tag{14a}$$

$$\mathbf{R}_{j+1}(\lambda_{j+1}) = \mathbf{R} + \lambda_{j+1}\mathbf{W}^T\mathbf{W}. \tag{14b}$$

Moreover, $\lambda_{j+1} \to +\infty$ as $j \to \infty$.

Proof. See (Son et al., 2013).

Consequently, $\|\mathbf{Q}_{j+1}\|$ converges to $\|\mathbf{Q}\|$, while $\|\mathbf{R}_{j+1}\|$ continuously increases to very large values. The ILC convergence speed decreases as the trial number increases. In order to avoid a continuous decrease of convergence speed in the trial domain, λ_{j+1} in the equivalent algorithm (14) can be fixed to a value that yields a sufficiently large updated weight $\|\mathbf{R}_{j+1}\|$, i.e. $\|\mathbf{R}_{j+1}\| \approx 10^6\|\mathbf{R}\|$, and $\|\mathbf{Q}_{j+1}\| \approx \|\mathbf{Q}\|$.

Remark 3.1. When the uncertainty is very small, i.e. $\|\mathbf{W}\| \approx 0$, the updated weights are approximately equal to the given $\mathbf{Q}$ and $\mathbf{R}$ which means that the robust ILC design is analogous to classical ILC. The larger $\mathbf{W}$, the larger λ_{j+1}, resulting in larger $\|\mathbf{R}_{j+1}\|$ and in smaller $\|\mathbf{Q}_{j+1}\|$ closer to $\|\mathbf{Q}\|$. Thus, the convergence speed is lower.

Remark 3.2. In the robust ILC (13), input constraints can be considered by the following constrained optimization problem, which is still a convex problem, i.e.

$$\begin{aligned} \underset{\mathbf{u}_{j+1},\lambda_{j+1}}{\text{minimize}} \quad & J_{\text{dual}}(\mathbf{u}_{j+1}, \lambda_{j+1}) \\ \text{subject to} \quad & \lambda_{j+1}\mathbf{I} - \mathbf{Q} \succeq 0 \\ & \mathbf{Q}\hat{\mathbf{e}}_{j+1} \in \mathcal{R}\left(\mathbf{Q} - \lambda_{j+1}\mathbf{I}\right) \\ & \|\mathbf{u}_{j+1}\|_\infty \leq \overline{u} \\ & \|\boldsymbol{\delta}\mathbf{u}_{j+1}\|_\infty \leq \overline{\delta u}, \end{aligned} \tag{15}$$

where inequality constraints on $u_{j+1}(k)$ and $\delta u_{j+1}(k) = u_{j+1}(k) - u_{j+1}(k-1)$ are taken into account to avoid actuator saturation.

4. EXPERIMENTAL VALIDATION ON AN OVERHEAD CRANE

The presented robust ILC algorithm is implemented and evaluated experimentally on a lab scale overhead crane. We also compare our robust ILC with the classical norm-optimal ILC and zero-phase low-pass filter ILC designs. The objective is to examine the properties of the ILC methods for two different levels of uncertainty. Therefore two models of the setup are considered: an inaccurate model with large uncertainty weight and an accurate model with small uncertainty weight. This section consists of three main parts. The first part describes the system and experimental setup. The second part discusses the implementation and comparison of the robust ILC, classical norm-optimal ILC, and zero-phase low-pass filter ILC based on the accurate model. Finally, part three repeats the comparison with the inaccurate model.

4.1 System Formulation

System descriptions: The overhead crane is shown in Figure 1 and drawn schematically in Figure 2. The position

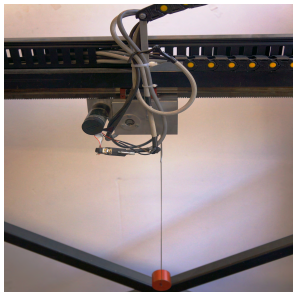

Fig. 1. Picture of the lab scale overhead crane

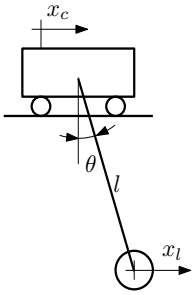

Fig. 2. Schematic representation

of the cart and the load are denoted by x_c [m] and x_l [m], respectively. The length of the cable, which is fixed, is denoted by l [m]. The angle of the load with respect to the vertical is θ [rad]. The single input u [V] is the command sent to the cart velocity controller. The single output is the load position, which is calculated as $x_l = x_c + l\sin\theta$. The encoder on the cart measures the cart position x_c, and another encoder measures θ. The angle is assumed small, i.e. $\sin\theta \approx \theta$, thus the load position can be approximated by $x_l = x_c + l\theta$. The system is sampled at 100 Hz. The input and the input rate of variation defined as $\delta u(k) = u(k) - u(k-1)$ are limited to the ranges $[-0.8,\ 0.8]$ V and $[-0.05,\ 0.05]$ V respectively, in order to avoid saturation of the velocity controller.

System models: If we neglect friction forces, the continuous time transfer function relating input u to load position x_l equals:

$$\frac{X_l(s)}{U(s)} = \frac{Ag}{s(ls^2 + g)}, \tag{16}$$

where $A = -0.6$, $g = 9.8\text{m/s}^2$, and the cable length l is 45.5cm. There are two models that are used in the experiment: an inaccurate model and an accurate model. First, in order to derive the inaccurate model with large uncertainty weight, the cable length l is assumed to be 65cm in the analytical model (16). The zero-order-hold discrete-time equivalent of this inaccurate model, $\hat{P}_{\text{inacc}}(z)$, is given by

$$\hat{P}_{\text{inacc}}(z) = \frac{-10^{-6}(1.508z^2 + 6.03z + 1.508)}{z^3 - 2.998z^2 + 2.998z - 1}. \tag{17}$$

Second, the accurate discrete-time system model $\hat{P}_{\text{acc}}(z)$ is derived using multisine excitation and frequency domain identification (Pintelon and Schoukens, 2001), yielding

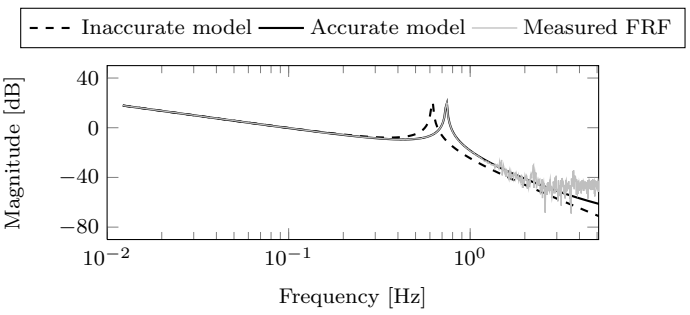

Fig. 3. Bode plots of measured frequency response function, and the accurate and inaccurate model

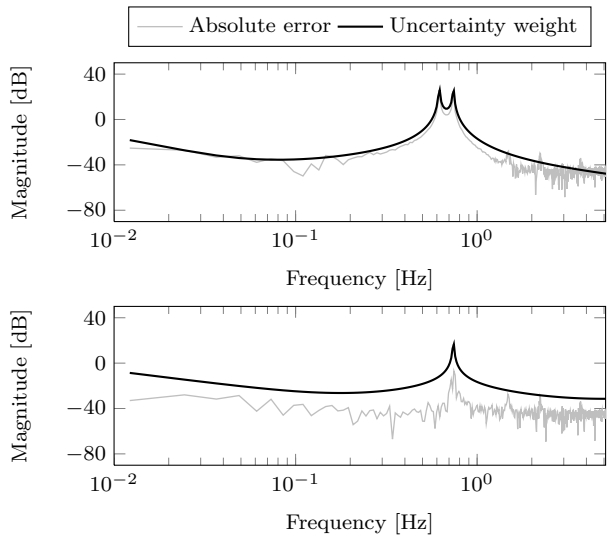

Fig. 4. Additive uncertainty weights for the inaccurate model (upper) and accurate model (lower) w.r.t. the absolute error

$$\hat{P}_{\text{acc}}(z) = \frac{0.0001448z^2 - 0.0003015z + 0.0001438}{z^3 - 2.998z^2 + 2.997z - 0.9998}. \quad (18)$$

The frequency responses of the inaccurate model and the accurate model are shown in Fig. 3, along with the measured frequency response function (FRF). The additive uncertainty weight corresponding to both models is obtained by manually tuning a stable transfer function that is an upper bound on the difference between the measured FRF and the system models, shown in Fig. 4.

Control objectives: The aim of the experiments is to track a reference trajectory, shown in Fig. 5, considering input constraints: $|u(k)| \leq 0.8$ V and $|\delta u(k)| \leq 0.05$ V.

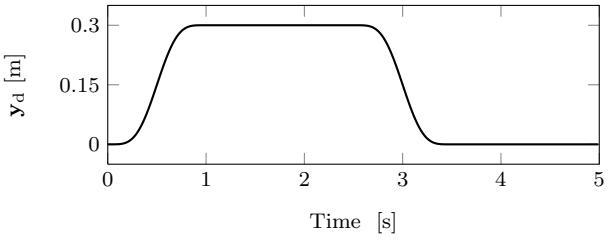

Fig. 5. Reference output

Robust ILC and classical norm-optimal ILC: First the discrete-time system model derived from the inaccurate model, the accurate model and the uncertainty weights are lifted with $N = 500$ samples, yielding $\hat{\mathbf{P}}$ and $\mathbf{W}$. Next, the weight parameters of both controllers are designed as follows:

- The weight $\mathbf{Q}$ determines the transient and converged performance errors. $\mathbf{Q}$ is selected as an identity matrix, i.e. $\mathbf{Q} = \mathbf{I}$ for an equal weight on all time samples.
- The weight $\mathbf{R}$ determines the convergence speed, and $\|\mathbf{R}\| > 0$ is used to be robust against trial-varying effects such as random disturbances and initial conditions. We select $\mathbf{R} = 10^{-6}\mathbf{I}$ for fast convergence speed purposes.
- The weight $\mathbf{S}$ is selected as $\mathbf{S} = \mathbf{0}$ for the smallest possible steady state error.

In order to deal with input constraints, the constraints $\|\mathbf{u}_{j+1}\|_\infty \leq 0.8$ and $\|\boldsymbol{\delta}\mathbf{u}_{j+1}\|_\infty \leq 0.05$ are imposed in both robust ILC algorithm (15) and classical norm-optimal ILC algorithm (8).

Zero-phase low-pass filter ILC: The zero-phase low-pass filter ILC approach is an ILC design that can cope with high frequency un-modelled dynamics (Longman, 2000). The main idea of zero-phase low-pass filter ILC is to achieve robustness by turning off the learning process at frequencies above a certain cut-off frequency, without introducing lag. First, a low-pass Butterworth filter is designed based on the selected cut-off frequency and order. Then, in order to achieve zero-phase filtering, the filter is applied forward and backward to the signal, which is similar to the MATLAB *filtfilt* filtering command. Finally, the zero-phase low-pass filter is combined with the classical norm-optimal ILC algorithm. The filter cut-off frequency in the inaccurate and the accurate model case is chosen as 0.4775Hz and 1.4324Hz, respectively, which is just below the first peak of the respective estimated uncertainties (see Fig. 4).

4.2 Experiment 1: Accurate system model

This subsection evaluates the robust ILC, classical norm-optimal ILC, and zero-phase low-pass filter ILC designs, all using the accurate model (18). The experimental results are shown in Fig. 6, Fig. 7 and Fig. 8.

Fig. 6 demonstrates that both robust ILC and classical norm-optimal ILC can achieve monotonic convergence and similar steady state error ($\mathbf{e}_\infty \approx 0.1$), while the convergence speed of robust ILC is slightly lower than for classical ILC design, especially in the first 5 trials. The difference in convergence speed is explained by the compromise between robustness and convergence speed in the robust algorithm. The tracking errors of the load at the 10th trial are shown in Fig. 7. The remaining error is mainly the result of the impulse input constraints (see Fig. 8). Other important sources of this error are trial-varying effects such as random disturbances and a non-zero initial load angle which is difficult to realise because of the low system damping.

Fig. 6 and Fig. 7 also show that the zero-phase low-pass filter ILC achieves monotonic convergence; however, this approach produces a significantly large steady state error

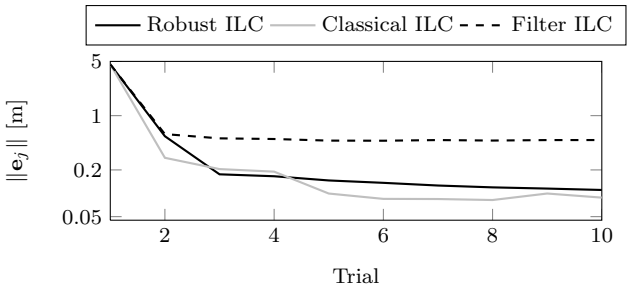

Fig. 6. Tracking errors in trial domain of the ILC controllers for the accurate model

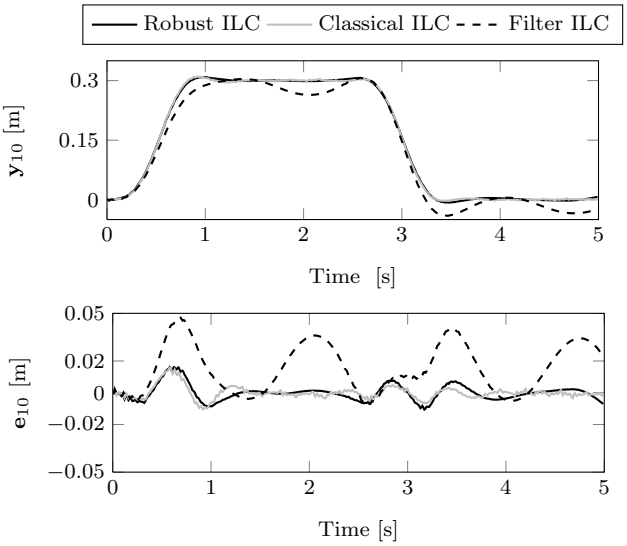

Fig. 7. Output and error signals at the 10th trial

compared to both robust ILC and classical norm-optimal ILC.

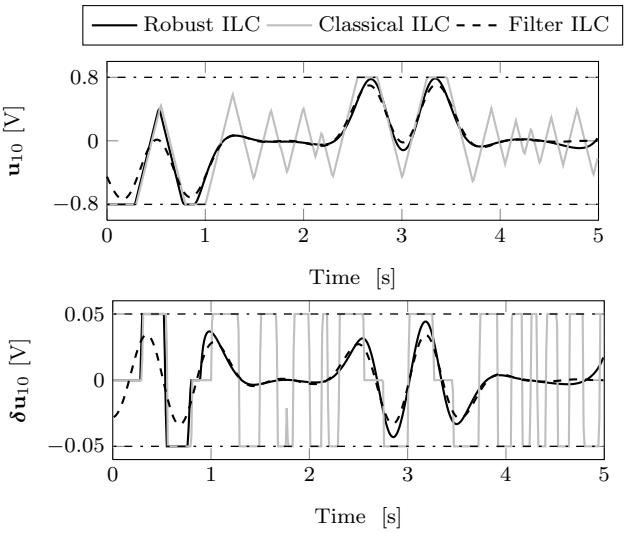

Fig. 8. Input and input rate signals at the 10th trial with constraints (dash-dotted line)

In addition, Fig. 8 shows the input and input rate signals at the 10th trial. The figure illustrates that the input signal of both robust ILC and classical norm-optimal ILC hit the constraints, while this is not the case for the input of low-pass filter ILC. Moreover, the input of the robust ILC is significantly smoother than the input of the classical ILC. This can be explained by the fact that the robust ILC learning speed is lower than the classical design, especially at high frequencies, and hence the input of the robust ILC has not yet converged completely at the 10th trial. Clearly, the robust input signal is more desirable in this case, because it causes less oscillations as shown in Fig. 7.

4.3 Experiment 2: Inaccurate system model

This part compares the robust ILC, classical norm-optimal ILC, and zero-phase low-pass filter ILC using the inaccurate model (17). The system uncertainty and corresponding uncertainty weight are now substantially larger than in the previous case. The experimental results are shown in Fig. 9, Fig. 10, and Fig. 11.

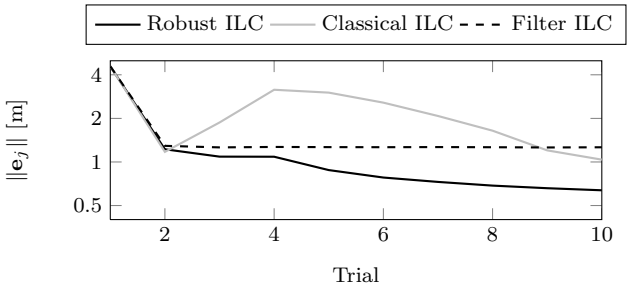

Fig. 9. Tracking errors in trial domain of the ILC controllers for the inaccurate model

From the results in Fig. 9, it can be seen that the classical norm-optimal ILC shows divergence of the tracking error after 3 trials. In contrast, the proposed robust ILC yields monotonic convergence of the tracking error, and this error still keeps decreasing after 10 trials. Fig. 10 shows the output and error signals of both approaches at the 4th trial, where the load swings excessively in the classical design. Clearly, this demonstrates the main advantage of the robust ILC design over the classical ILC: the robust ILC can achieve monotonic convergence even for large uncertainty. From the 5th trial of the robust controller, the equivalent norm-optimal ILC approach (14) is applied with $\lambda_{j+1} = 1.1$, which corresponds to $\|\mathbf{R}_{j+1}\| = 3.6 \times 10^6 \|\mathbf{R}\|$ and $\|\mathbf{Q}_{j+1}\| \approx \|\mathbf{Q}\|$, in order to obtain a faster convergence speed. The output and error signals at the 10th trial are shown in Fig. 11, showing an improvement with respect to the 4th trial.

Fig. 9, Fig. 10, and Fig. 11 also show the performance of the zero-phase low-pass filter ILC. Compared to the classical norm-optimal ILC, using the filter approach avoids divergence of error at the 3rd trial, and yields monotonic convergence. However, the performance of the robust ILC design is still significantly better than the zero-phase low-pass filter ILC.

An additional simulation analysis, assuming the true system is the accurate model, shows that the robust ILC error converges monotonically to a steady state error that is comparable to the results shown in Fig. 6, i.e. $\|\mathbf{e}_\infty\| \to 0.1$. The classical ILC error converges to the same steady state error with higher convergence speed; however, bad transient learning is observed. Finally, the low-pass filter ILC converges monotonically to a larger steady state error that is comparable to the error at the 10th trial shown in Fig. 9 (dashed line).

5. CONCLUSION

A robust norm-optimal ILC design has been experimentally validated and compared with classical norm-optimal ILC and zero-phase low-pass filter ILC on a lab scale overhead crane. Two system models with different levels of uncertainty were considered. For the model with large uncertainty, the experimental results show that the classical norm-optimal ILC design yields divergence of tracking error while the robust ILC design achieves monotonic convergence. Adding a zero-phase low-pass filter helps the

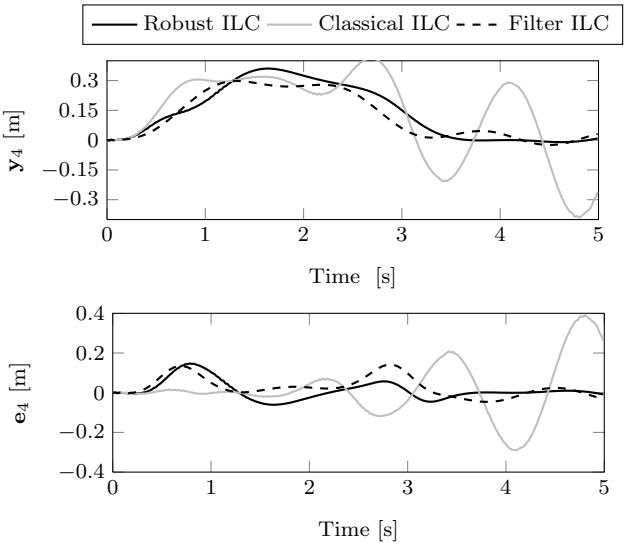

Fig. 10. Output and error signals at the 4th trial

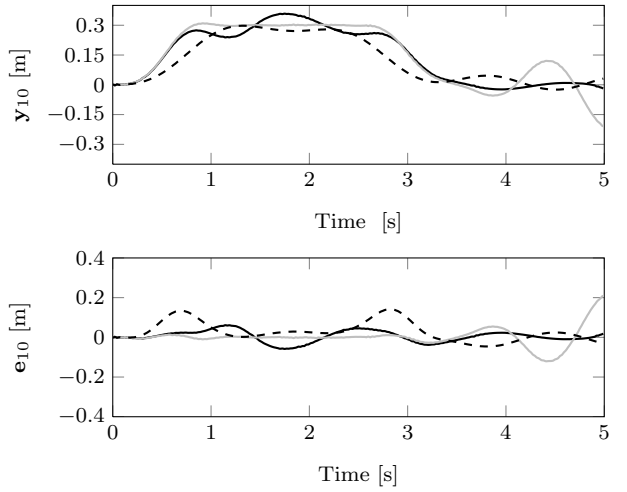

Fig. 11. Output and error signals at the 10th trial

classical ILC to avoid divergence, however at the cost of larger converged tracking error than the proposed robust ILC. For the model with small uncertainty, both the classical ILC and robust ILC achieve monotonic convergence with similar converged performance.

REFERENCES

Ahn, H.S., Chen, Y., and Moore, K. (2007). Iterative learning control: Brief survey and categorization. *Part C: Applications and Reviews, IEEE Transactions on Systems, Man, and Cybernetics*, 37(6), 1099 –1121.

Ahn, H.S., Moore, K., and Chen, Y. (2006). Monotonic convergent iterative learning controller design based on interval model conversion. *IEEE Transactions on Automatic Control*, 51(2), 366–371.

Bristow, D. and Alleyne, A. (2008). Monotonic convergence of iterative learning control for uncertain systems using a time-varying filter. *Automatic Control, IEEE Transactions on*, 53(2), 582–585.

Bristow, D.A., Tharayil, M., and Alleyne, A.G. (2006). A survey of iterative learning control: a learning based method for high-performance tracking control. *IEEE Control Systems Magazine*, 26, 96–114.

Donkers, T., van de Wijdeven, J., and Bosgra, O. (2008). Robustness against model uncertainties of norm optimal iterative learning control. In *Proceedings of the American Control Conference*.

Gunnarsson, S. and Mikael Norrlöf (2001). On the design of ILC algorithms using optimization. *Automatica*, 37(12), 2011–2016.

Haber, A., Fraanje, R., and Verhaegen, M. (2012). Linear computational complexity robust ilc for lifted systems. *Automatica*, 48(6), 1102 – 1110.

Longman, R.W. (2000). Iterative learning control and repetitive control for engineering practice. *International Journal of Control*, 73, 930–954.

Moore, K., Chen, Y., and Ahn, H.S. (2005). Algebraic $\mathcal{H}_\infty$ design of higher-order iterative learning controllers. In *Proceedings of the IEEE International Symposium on Intelligent Control*, 1207 –1212.

Norrlöf, M. and Gunnarsson, S. (2002). Time and frequency domain convergence properties in iterative learning control. *International Journal of Control*, 75(14), 1114–1126.

Owens, D. and Daley, S. (2008). Robust gradient iterative learning control: time and frequency domain conditions. *International Journal of Modelling, Identification and Control*, 4(4), 315–322.

Pintelon, R. and Schoukens, J. (2001). *System Identification: A Frequency Domain Approach*. Wiley-IEEE Press, New York.

Rogers, E., Lam, J., Galkowski, K., Xu, S., Wood, J., and Owens, D. (2001). LMI based stability analysis and controller design for a class of 2D discrete linear systems. In *Proceedings of the 40th IEEE Conference on Decision and Control*, volume 5, 4457–4462.

Roover, D. (1996). Synthesis of a robust iterative learning controller using an $\mathcal{H}_\infty$ approach. In *Proceedings of the 35th IEEE Conference on Decision and Control*, volume 3, 3044–3049.

Son, T.D., Pipeleers, G., and Swevers, J. (2013). Robust optimal iterative learning control with model uncertainty. In *Proceedings of the 52nd IEEE Conference on Decision and Control*. Florence, Italy.

van de Wijdeven, J.J.M., Donkers, M.C.F., and Bosgra, O.H. (2011). Iterative learning control for uncertain systems: Noncausal finite time interval robust control design. *International Journal of Robust and Nonlinear Control*, 21(14), 1645–1666.

ACKNOWLEDGEMENTS

This work was supported by the European Commission under the EU Framework 7 funded Marie Curie Initial Training Network (ITN) IMESCON (grant no. 264672). This work also benefits from the IWT-SBO 80032 (LECOPRO) project of the Institute for the Promotion of Innovation through Science and Technology in Flanders (IWT-Vlaanderen), from KU Leuven-BOF PFV/10/002 Cente of Excellence: Optimization in Engineering (OPTEC), and from the Belgian Network Dynamical Systems, Control and Optimization (DYSCO), initiated by the Belgian Science Policy Office. Goele Pipeleers is Postdoctoral Fellow of the Research Foundation Flanders (FWO).